Crystal Structure Directed Catalysis by Aluminium Metal-Organic Framework: Mechanistic Insight into the Role of Coordination of Al Sites and Entrance Size of Catalytic Pocket

Ayan Maity,[1#] Baljeet Singh,[1#] Kshama Sharma,[2] Subhradip Paul,[3] P. K. Madhu,[1,2*] and Vivek Polshettiwar[1*]

[1]Department of Chemical Sciences, Tata Institute of Fundamental Research (TIFR), Mumbai, India. Email: vivekpol@tifr.res.in,

[2]TIFR Centre for Interdisciplinary Sciences, TIFR Hyderabad, India. madhu@tifr.res.in

[3]Sir Peter Mansfield Imaging Centre, School of Physics & Astronomy, University of Nottingham, Nottingham, UK.

Methods

Synthesis of Al-BTC MOFs:

Synthesis of M100 MOF. $Al(NO_3)_3.9H_2O$ (0.63 gm) and P123 (1 gm) were dissolved in 25 ml of water. Trimesic acid (BTC) (0.56 gm) was dissolved in 27 mL of ethanol separately and stirred for 30 minutes at room temperature. The above two solutions were mixed and stirred further for 30 minutes at room temperature and then transferred to a 60 mL Teflon sealed microwave reactor and exposed to microwaves at 120 ℃ for 2 hours. After cooling the reaction mixture, the product was isolated by centrifugation and washed several times with water and ethanol to remove the unreacted starting materials. The white powder Al-MOF was then dried under vacuum.

Synthesis of M96 MOF. $Al(NO_3)_3.9H_2O$ (0.63 gm) and BTC (0.56 gm) were dissolved in a mixture of water (40 mL), ethanol (10 mL) and DMF (10 mL) and stirred for 30 minutes at room temperature. This solution was then transferred to a 60 mL Teflon sealed microwave reactor and microwaved at 150 ℃ for 1 hour. After cooling the reaction mixture, the product was isolated by centrifugation and washed several times with water and ethanol to remove the unreacted starting materials. The white powder Al-MOF was then dried under vacuum.

Catalysis: Both MOFs were evaluated for their catalytic activity before as well as after activation at 120 °C for 4 hours under vacuum. 210 mg of 4-chlorobenzaldehyde (PCB) and 40 mg of Al-MOF (before activation) was taken in 10 mL of dry methanol in the inter atmosphere and the reaction mixture was stirred at 50°C for 4 hours. For activated MOFs, there were first heated at 120 °C for 4 hours under vacuum in Schleck tube and then cooled to 50°C under nitrogen. Methanol and PCB were then added to the reactor and stirred at 50°C for 4 hours. Products were identified by gas chromatography-mass spectroscopy.

Characterization of Al-BTC MOFs:

All the materials were characterized by scanning electron microscopy (SEM), transmission electron microscopy (TEM), powder X-ray diffraction and N_2 sorption analysis. Nitrogen adsorption-desorption isotherms were measured at -196 °C with a Micromeritics Flex 3 surface area and porosity analyser. Before the measurements, the samples were degassed in vacuum at 120 °C for 24 hours by using a degasser followed by 2 hours *in situ* degassing at the analyser port. The thermal stability of the sorbent was studied using thermogravimetric analysis (TGA) by heating the samples in a 70 mL alumina pan from 30 °C to 800 °C at a heating rate of 10 °C min^{-1} under an oxygen flow of 40 mL min^{-1}. The weight loss was calculated from 150 °C to 800 °C. Powder-XRD of all samples was recorded using a Panalytical Xpert Pro X-ray diffractometer using CuKα radiation (1.54 Å).

All solid-state NMR spectra were acquired on a Bruker-Avance 700 (16.7 T) NMR spectrometer using a 2.5 mm MAS probe with samples fully packed inside zirconium oxide rotors. The MAS spinning frequency was 20 kHz for the ^{27}Al single-pulse experiment and the ^{1}H-^{13}C cross-polarization (CP) experiments and 11.5 kHz for the ^{27}Al MQMAS experiment. Cross-polarization was achieved by setting the MAS Hartmann-Hahn matching condition, ^{13}C RF fields of ~ 50 kHz and ^{1}H radiofrequency amplitude to ~ 70 kHz (second sideband matching condition). The contact time for CP was kept at 3.25 ms, and 4096 transients were averaged with a recycle delay of 2 s. All ^{13}C spectra were acquired using 87.71 kHz $rCW^{ApA1,2}$ ^{1}H decoupling during an acquisition time of 20 ms. Data were processed using the NMRPipe Version 8.2[3] with exponential line broadening of 30 Hz. All spectra were referenced externally to tetramethylsilane (TMS) for ^{1}H (δ_{ref} = 0 ppm) and admantane for ^{13}C (δ_{ref} = 38.4 ppm for $–CH_2$ of admantane). For all ^{27}Al single-pulse experiments, the RF amplitude was such that the pulse length was 7.0 μs, and a recycle delay time of 1 s was employed with an acquisition time of 15 ms. The chemical shifts for ^{27}Al were referenced using 1 M aqueous $Al(NO_3)_3$ for ^{27}Al (δ_{ref} = 0 ppm). To gain better spectral resolution, MQMAS spectroscopy was performed on M96. The experimental details are presented in Table S4, Figure S11.

Multiple-quantum MAS (MQMAS) Spectroscopy. All spectra were acquired at 12 kHz MAS frequency, ~96 K, and 600 MHz (^{1}H Larmor frequency) on a Bruker spectrometer using a double-resonance cryoprobe[4]. Eighty hypercomplex[5] points were acquired in the indirect dimension with 1-2 s of recycle delay between each point. A total of 2048 points were acquired in the direct dimension. The recycle delay was determined by using a saturation recovery experiment in each case. The number of

transients was kept at 12N to complete the phase cycling for triple quantum selection on the conversion pulse. ^{1}H heteronuclear decoupling during indirect and direct dimensions were carried out employing SW_f –TPPM[6,7]with an RF amplitude of 100 kHz. For ^{27}Al RF amplitude calibration and spectral referencing, a frozen solution of $AlCl_3.9H_2O$ was used. The hard pulses used for MQ excitation and 3Q reconversion were of RF amplitude 100 kHz, while the soft pulse for selection of the central transition was of RF amplitude 30 kHz. The amplitudes here are that of the RF fields in the coil and not of the transitions. In addition, 20 μs of z-filter was used in between the hard pulse for conversion and the soft pulse for central transition selection. A shearing transformation was carried out in Bruker Topspin, and the spectra were referenced with respect to the $AlCl_3.9H_2O$ signal. The indirect dimension was referenced according to the convention Cz as given in Ref. 8 and 9. An exponential apodisation of 100 Hz was used in both dimensions.

HETCOR Spectroscopy. ^{1}H-^{27}Al HETCOR solid-state NMR spectra of samples were acquired on a Bruker AVANCE 500 NMR spectrometer (11.8 T) using a 4 mm MAS probe with samples fully packed in the rotors. All experiments were recorded at MAS frequency of 8.33 kHz. 2D spectra were acquired with 80 scans for each of the 160 t_1 increments with a recycle delay of 2 s. The CP contact time was kept as 1 ms. rCW^{ApA} heteronuclear decoupling was applied during t_2 with an RF amplitude of 85 kHz. STATES-TPPI was used for frequency discrimination in the indirect dimension. Data were processed using Topspin 3.5 with an exponential line broadening of 50 Hz which were edited using inkscape 0.92.

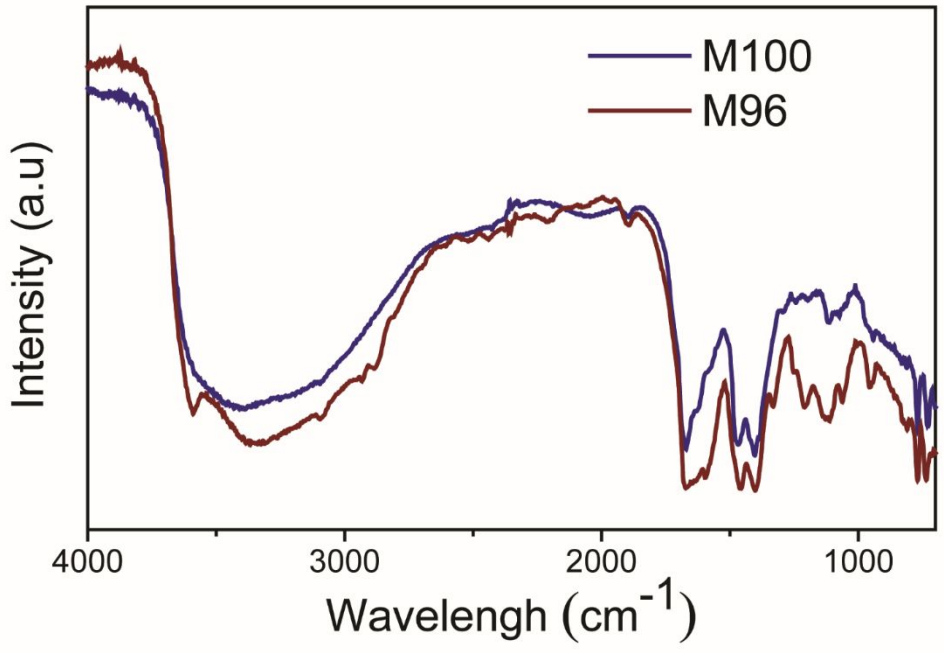

Figure S1. FTIR specta of M100 and M96

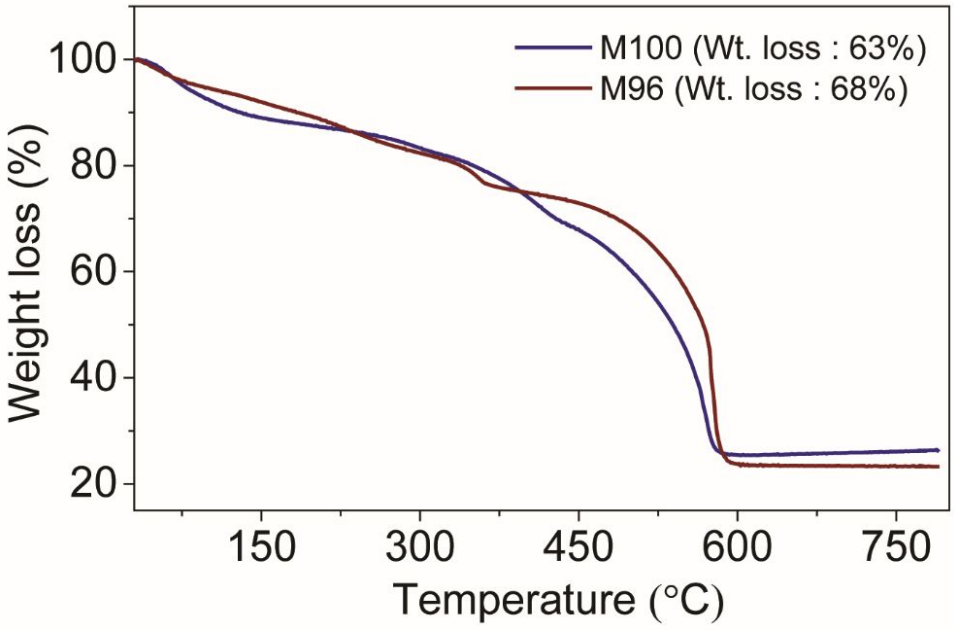

Figure S2. TGA profiles of M100, and M96.

Table S1. The TGA weight loss, EXD elemental analysis of both the MOFs.

Sample Name	TGA Weight Loss (wt. %)	EDX Elelemental Analysis (weight %)		
		C	O	Al
M100	63.0±3	44.2	46.6	9.1
M96	68.0±2	41.5	46.4	12.0

Standard error in SEM EDX elemental analysis ± 10 %

Figure S3. Crystal structure of MIL-100 (Al) Reproduced from Ref. 13

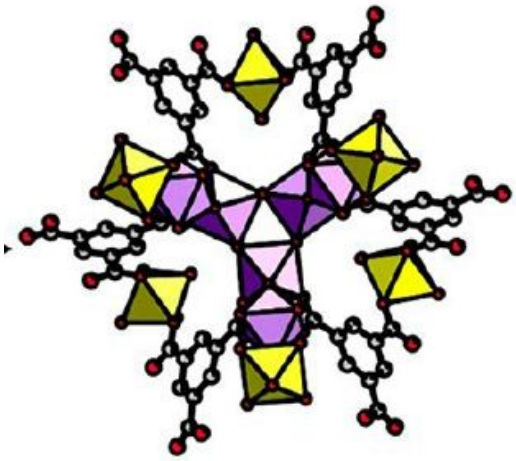

Figure S4. Crystal structure of MIL-96 (Al) Reproduced from Ref. 15

Table S2. HK pore size distribution analysis of M100 and M96 Al-MOFs

Al-MOF	Pore Size (Å)	Pore Volume (cm^3/g)
M100	Total	0.93
	Total (simulated)	0.94
	Cavity A (5±1)	0.39
	Cavity B (9.5±4)	0.55
M96	Total	0.41
	Total (simulated)	0.38
	Cavity A (4.5±1)	0.08
	Cavity B (5.8±1.5)	0.16
	Cavity C (9.7±2.3)	0.14

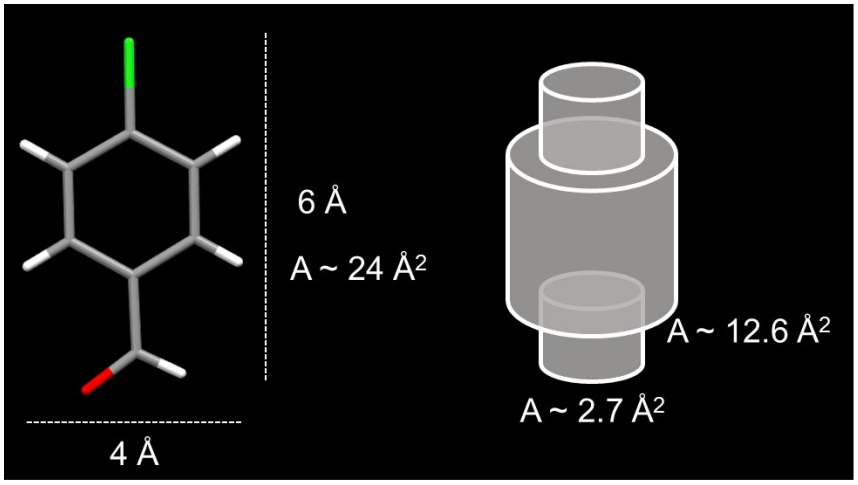

Figure S5. Molecular size of p-chloro benzaldehyde (PCB) in its monomeric form without any solvation

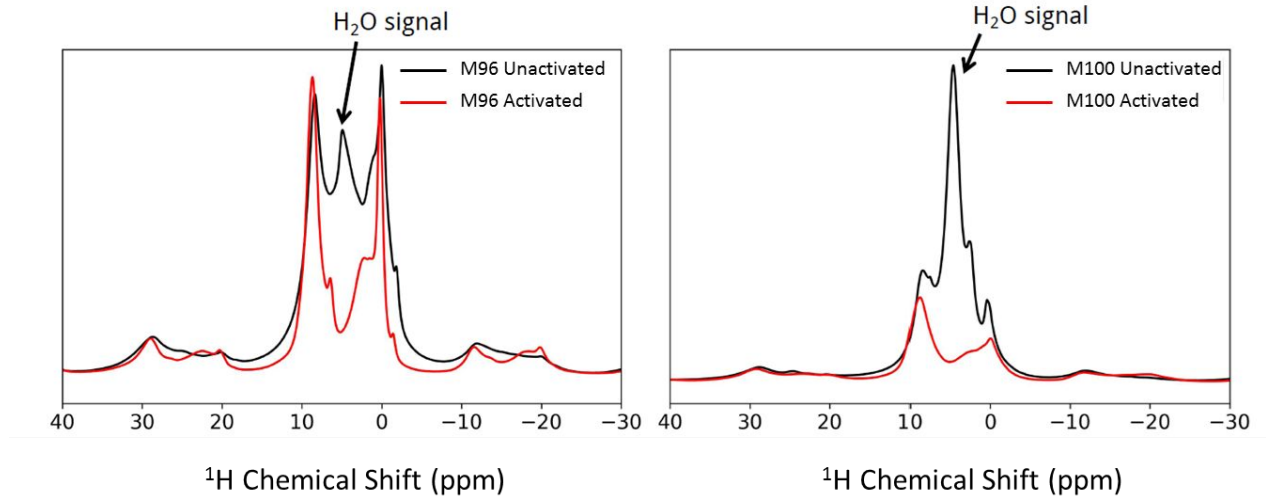

Figure S6. ^{1}H MAS NMR of all Al-MOFs before and after activation

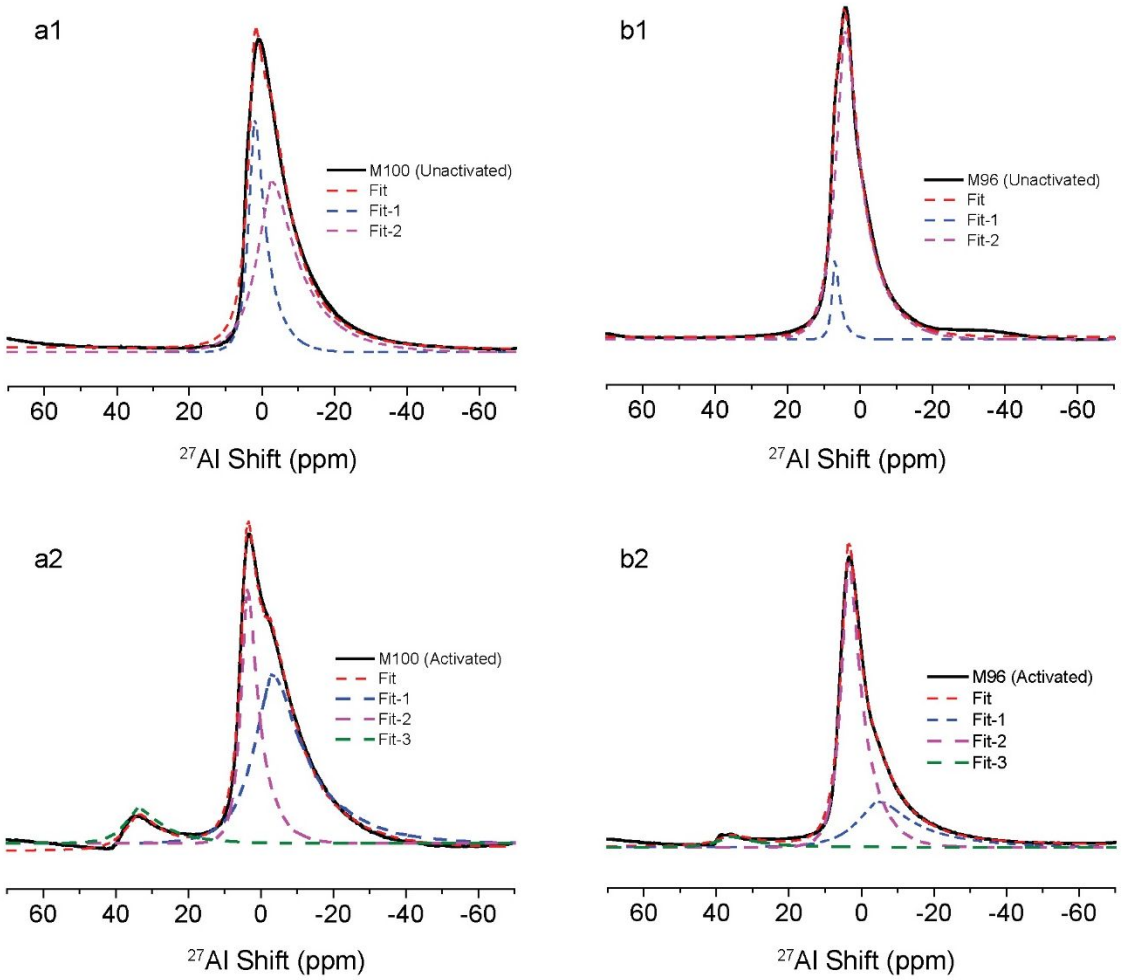

Figure S7. ^{27}Al direct excitation MAS spectra of MOF samples. Deconvolution of the spectra was performed using the Czjzek model using DMFIT. The fits were done assuming that the lines are inhomogeneously broadened. The critical exponent of the Czjzek distribution was assumed such that it resembles Gaussian isotropic distribution of the EFG tensor elements[10].

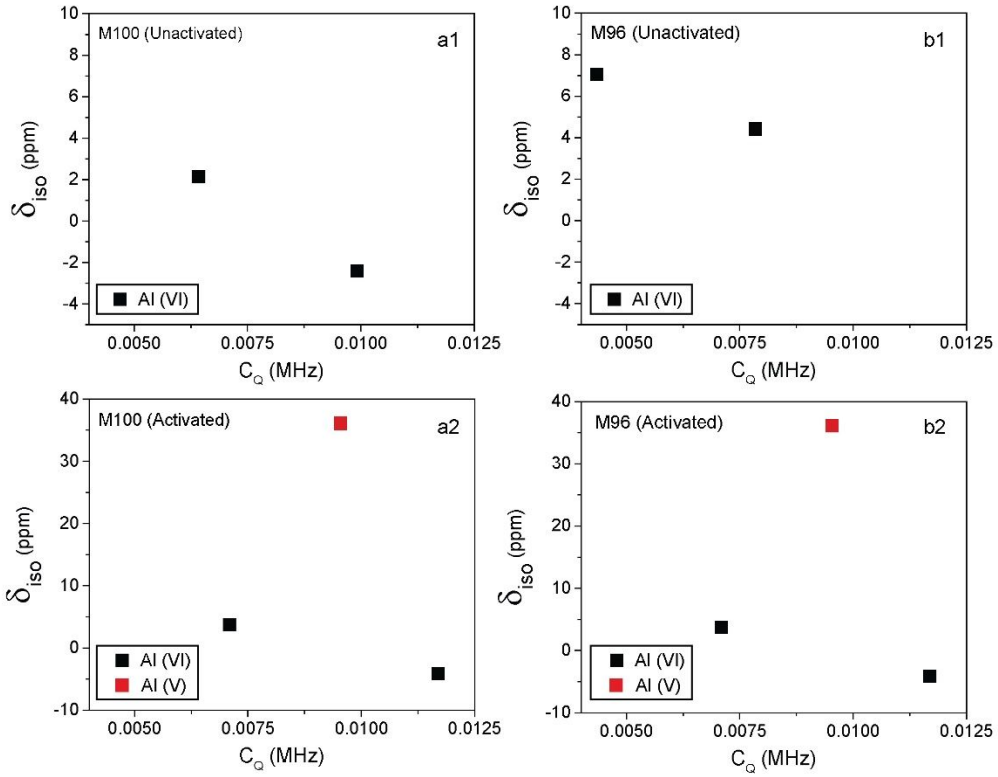

Figure S8. Plot of isotropic chemical shift (δ_{iso}) against quadrupolar coupling constant (C_Q, MHz) (a1) M100 (unactivated) (a2) M100 (activated) (b1) M96 (unactivated) (b2) M96 (activated).

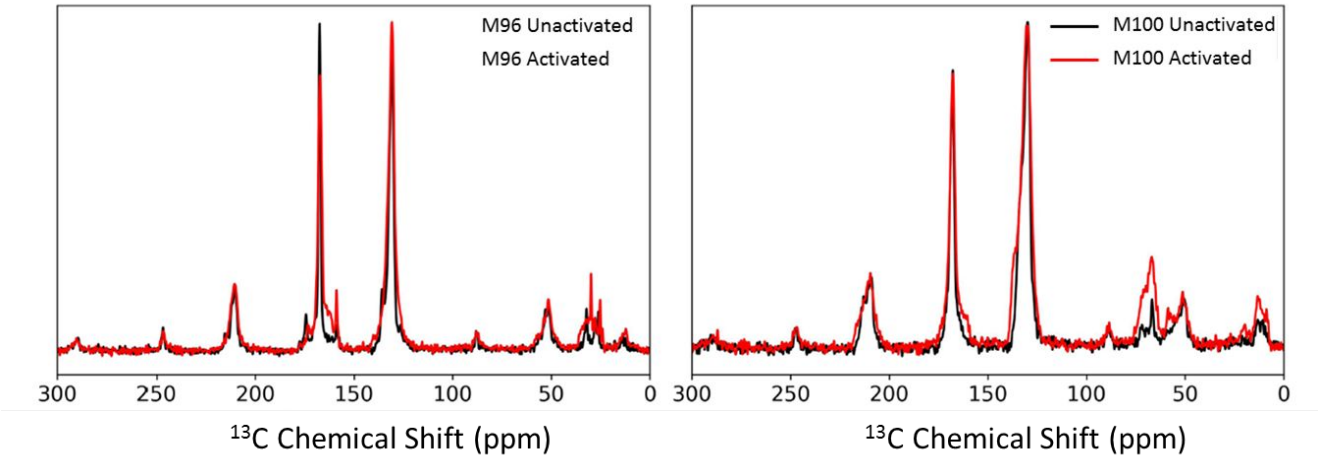

Figure S9. ^{13}C MAS NMR of all Al-MOFs before and after activation

Table S3. T_2 analysis of the Al-MOFs before and after activation.

M96 (unactivated)		M96 (activated)	
Peak Position (ppm)	T_2 (ms)	Peak Position (ppm)	T_2 (ms)
130	0.930	130	0.737
167	1.983	167	1.135
M100 (unactivated)		M100 (activated)	
Peak Position (ppm)	T_2 (ms)	Peak Position (ppm)	T_2 (ms)
130	0.530	130	0.444
167	1.067	167	0.850

The group of signals located in the chemical shift range of 130-145 ppm is assigned to the aromatic carbons of the BTC ligand, and the others in the range of 167-172 ppm are assigned to the carbonyl of carboxylic (–COO) group of the BTC ligands.

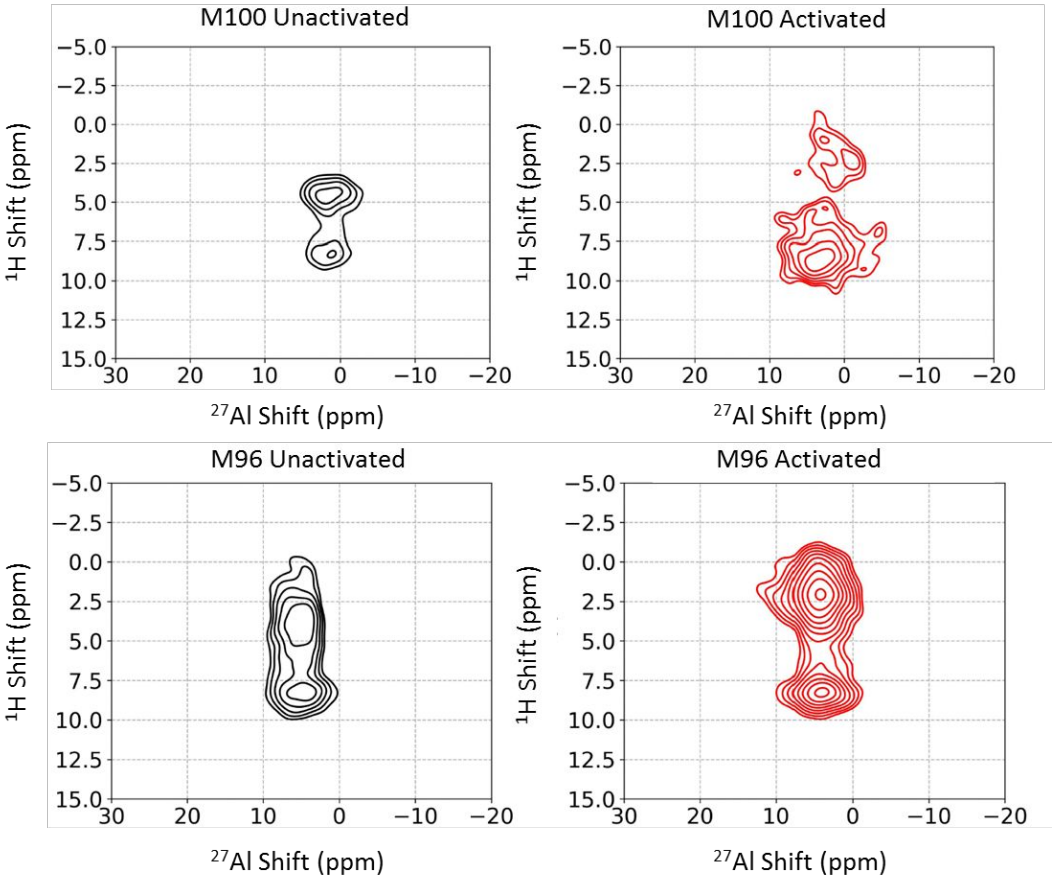

Figure S10. ^{1}H-^{27}Al HETCOR spectra of the Al MOFs before and after activation

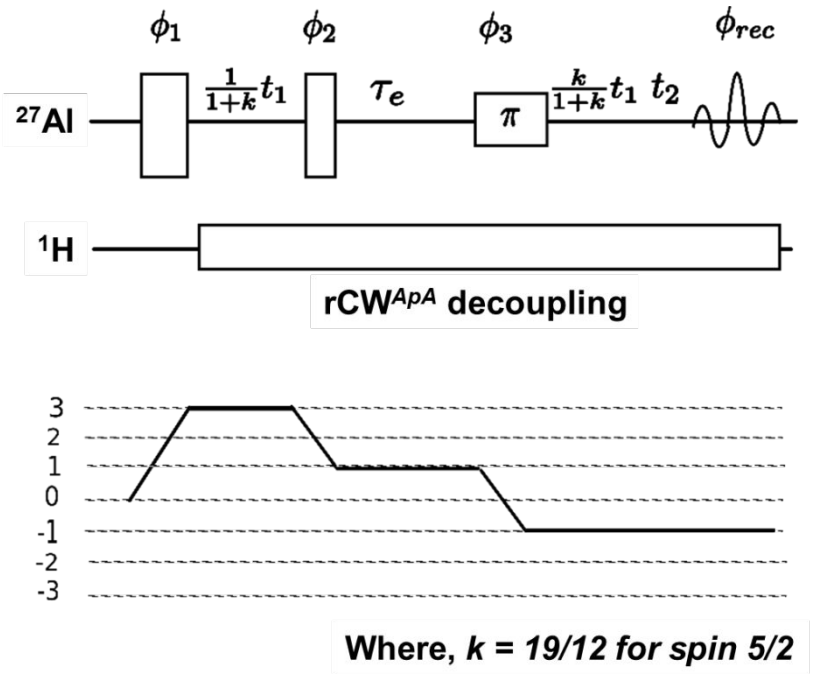

Figure S11. 2D ^{27}Al 3QMAS split-t_1-shifted-echo scheme.

Table S4. Experimental details used to acquire 2D 3QMAS experiment ^{27}Al NMR spectra

Experimental Parameters	Spectrometer Frequency: 700 MHz
Pulse length with phase ϕ_1 (μs)	8.0
Pulse length with phase ϕ_2 (μs)	2.0
Pulse length with phase ϕ_3 (μs)	15.0
Spectral width (F_1) (kHz)	40.0
Spectral width (F_2) (kHz)	80.0
Number of scans	48
No. of increments in indirect dimension	280
Recycle delay (s)	1.0

References:

1. Equbal, A.; Bjerring, M.; Madhu, P. K.; Nielsen, N. C. Improving spectral resolution in biological solid-state NMR using phase-alternated rCW heteronuclear decoupling. Chem. Phys. Lett.635, 339 (2015).
2. Godburt, A.; Madhu, P. K. Multiple-quantum magic-angle spinning: High-resolution NMR spectroscopy of half-integer spin quadrupolar nuclei. *Ann. Rep. NMR. Spec*. **2005**, *54*, 81-153.
3. Delaglio, F.; Grzesiek, S.; Vuister, G. W.; Zhu, G.; Pfeifer, J.; Bax, A. NMRPipe: A multidimensional spectral processing system based on UNIX pipes, J. Biomol. NMR, 6, (1995), 277-293.
4. Medek, A.; Harwood, J. S.; Frydman, L. Multiple-Quantum magic-angle spinning NMR: A new method for the study of quadrupolar nuclei in solids. *J. Am. Chem. Soc*. **1995**, 117, 12779-12787.
5. Marion, D.; Wüthrich, K. Application of phase sensitive two-dimensional correlated spectroscopy (COSY) for measurements of 1H-1H spin-spin coupling constants in proteins. *Biochem. Biophys. Res. Commun.* **1983**, *113*, 967-974.
6. Thakur, R.; Kurur, N.; Madhu, P. Swept-frequency two-pulse phase modulation for heteronuclear dipolar decoupling in solid-state NMR. *Chem. Phys. Lett.* **2006**, *426*, 459-463.
7. Paul, S.; Kurur, N. D.; Madhu, P. K. On the choice of heteronuclear dipolar decoupling scheme in solid-state NMR. *J. Magn. Reson.* **2010**, *207*, 140-148.
8. Hanaya M.; Harris, R. K. Optimization of Two-Dimensional Multiple-Quantum MAS NMR Experiments for I = 3 / 2 Nuclei on a Moderate-Field Spectrometer. *J. Phy. Chem. A.* **1997**, *101*, 6903-6910.
9. Man, P. P. Scaling and labeling the high-resolution isotropic axis of two-dimensional multiple-quantum magic-angle-spinning spectra of halfinteger quadrupole spins. *Phy. Rev. B*, **1998**, *58*, 2764-2782.
10. Wischert, R.; Florian, P.; Copéret, C.; Massiot, D.; Sautet, P. MAS NMR spectra of quadrupolar nuclei in disordered solids: The Czjzek model *J. Phys. Chem. C* **2014**, *118*, 15292−15299.